11 SCIENTIFIC HIGHLIGHT OF THE MONTH

OPTIMIZING STRUCTURE FOR LARGER, FINITE SYSTEMS

Michael Springborg, Jan-Ole Joswig, Valeri G. Grigoryan, Christian Gräf, Sudip Roy, and Pranab Sarkar

Physical Chemistry, University of Saarland, D – 66123 Saarbrücken, Germany

http://www.uni-saarland.de/fak8/springborg/home.html

ABSTRACT

The problems related to the calculation of structure of larger, finite systems are discussed in detail. In particular, it is emphasized *i*) that a complete search in the multidimensional structure space for a given system is without reach for any but the absolutely smallest systems, *ii*) that systematic studies of more systems without severe assumptions about their structure not are possible with current parameter-free electronic-structure methods, and *iii*) that one has to rely on different kinds of 'dirty tricks' in order to calculate the properties of interest. With the embedded-atom method combined with an '*aufbau/abbau*' approach (described in the text) we study structural and energetical properties of metal clusters, whereas for semiconductor nanoparticles we use a tight-binding method in combination with the assumption that their structure can be derived from the wurtzite or zincblende crystal structure. Finally, we study the properties of a series of Ti_mC_n metcars for which we apply a genetic algorithm in the structure optimization in combination with the tight-binding method for the electronic-structure calculation.

1. INTRODUCTION

The problems we shall address in this paper may be best described through an example taken from some recent experimental studies at the University of Konstanz in Germany.

About 10 years ago the group around Castleman in Pennsylvania produced metal-containing carbon clusters M_mC_n. In mass abundance spectra they observed a peak for $(m,n) = (8,12)$ with M being Ti [1], suggesting that this cluster was particularly stable. They proposed a cage-like structure of cubic T_h symmetry with 12 five-membered rings, each containing two metal and three carbon atoms. Thus, the topology is as that of the smallest possible fullerene molecule C_{20} but containing metal atoms. An alternative description of the structure is to consider it as formed by a cube of the eight metal atoms. The 12 carbon atoms forms six C_2 dimers that are placed symmetrically above the sides of the cube with the C–C bonds parallel to the edges. Later, theoretical studies – first of all by Dance [2] — suggested that the structure had tetragonal T_d symmetry. Compared with the T_h symmetry, the C_2 dimers are for the T_d symmetry lying parallel to the diagonals of the six sides of the cube of the eight metal atoms and, in addition, the cube becomes somewhat distorted. First recently, theoretical and experimental studies agree that the tetragonal structure is the correct one (see, e.g., [3]). In the meantime it has been found that also for other metals (e.g., Hf, Zr, V) those so-called metallocarbohedrenes or metcars can be formed, and even metcars with more different types of metals have been produced. However, whether they occur in significant amounts depend strongly on the experimental conditions, suggesting that kinetic effects play a significant role in their production.

In order to study the properties of the Ti-based material further, the group around Ganteför in Konstanz decided to study a whole class of M_mC_n clusters with different values of (m,n) centered around $(m,n) = (8,12)$ [4]. Using two different sources, Ti and C atoms were produced that subsequently were allowed to form the clusters mentioned above. After ionization, a magnetic field could be used to mass-separate the clusters and, finally, photoelectron spectra could be recorded for these mass-selected clusters. Accompanying theoretical studies would then be very useful as a support for the interpretation of the experimental results.

As one of the clusters of the experiments let us choose Ti_6C_{10}, i.e., $(m,n) = (6,10)$, whose structure is absolutely unknown. One *may* consider it as been formed by removing two carbon and two titanium atoms from the more famous $(m,n) = (8,12)$ cluster, but the first question is then: which four atoms shall be removed? Starting with the two proposed structures (i.e., those of T_h and T_d symmetry) for the $(m,n) = (8,12)$ cluster mentioned above we tried this strategy (using a computational method that will be described below) but obtained a new structure in each attempt. The simplest approach would then be to choose the structure of the lowest total energy. However, it has to be remembered that the experiment is performed in a completely different way: instead of starting with the larger $(m,n) = (8,12)$ cluster and from that removing some atoms, the $(m,n) = (6,10)$ cluster is formed from essentially isolated atoms and, therefore, it is not at all given that its structure has any resemblance to that of the $(m,n) = (8,12)$ cluster.

Thus, the first problem in this case is that we have essentially no information about the structure of the system of interest except for its composition but want nevertheless to calculate some of its properties. The second problem is that finite systems of the type A_N have a very rapidly growing

N	No. of structures
7	4
8	8
9	21
10	64
11	152
12	464
13	1328

Table 1: *No. of metastable structures for Lennard-Jones-Clusters LJ_N as a function of N. The results are from [5].*

number of metastable structures as a function of N. As a simple illustration we may consider N identical particles interacting via Lennard-Jones potentials. This system is so simple that it allows for exhaustive studies of the total-energy surface. Tsai and Jordan [5] have performed such studies and in Table 1 we show their results for the number of metastable structures as a function of N. It should be obvious that this number grows rapidly with N.

These problems become even more significant when one wants to study the semiconductor or metal nanoparticles that are of large experimental interest currently. For these the precise composition is often not known and, instead, one has often a certain size-distribution. Moreover, their diameters lie typically in the range 1–100 nm, meaning that the number of atoms per particle is from 100s to several 10 000s.

Studying such systems theoretically with electronic-structure methods one has therefore to be very precise in identifying which questions one attempts to address. For instance, when the so-called magic numbers (the values of N for which the clusters are particularly stable) are sought, it is important to have a good estimate of the lowest total energy for a given value of N, but it may not be necessary to identify the global total-energy minimum. On the other hand, for optical properties or the electron density of either some selected or of all orbitals a good approximation to the structure of the global total-energy minimum should be used, although the structure may not have to be that of a local or the global total-energy minimum. For vibrational properties it may be crucial to have identified the global total-energy minimum.

In the present contribution we shall describe some of the methods we are using in addressing these issues. Due to the size and low symmetry of the systems of our interest and to the large number of structures that have to be studied, we do not consider it possible to apply parameter-free first-principles electronic-structure methods but use approximate methods. For the sake of completeness these methods shall be described briefly in Sec. 2. Subsequently, we shall study different properties of elemental metal clusters in Sec. 3 and of semiconductor nanoparticles in Sec. 4. In Sec. 5 we shall return to the metcars, and a brief resumé is offered in Sec. 6.

2. ELECTRONIC-STRUCTURE METHODS

We use two parameterized methods in our studies of the properties of the nanoparticles.

According to conventional wisdom, the electrons in metallic systems are delocalized and, therefore, less sensitive to the precise positions of the nuclei. For metallic nanoparticles we use, of this reason, the embedded-atom method of Daw and Baskes [6, 7, 8, 9]. The basic idea behind this method is to consider each atom of a metal as an impurity embedded in a host of the rest of the atoms. This provides one contribution to the total energy of the system of interest. The other contribution comes from the interactions between the atoms which is written as a sum of pair potentials. Accordingly, the total energy has the following form

$$E_{\rm tot} = \sum_i F_i(\rho_i^h) + \frac{1}{2}\sum_{i\neq j}\phi_{ij}(R_{ij}). \tag{1}$$

Here, ρ_i^h is the electron density felt by the ith atom but coming from the other atoms. In principle, this density is structured but as a simplification we simply take the value at the site of the nucleus $\vec{R}_i$ of the superposition of the atomic electron densities from the other atoms,

$$\rho_i^h = \sum_{j\neq i}\rho_j^a(R_{ij}) \tag{2}$$

with

$$R_{ij} = |\vec{R}_i - \vec{R}_j|. \tag{3}$$

Using this method requires information on the embedding functions F_i, the pair interactions ϕ_{ij}, and the atomic electron densities ρ_j^a. The latter have been obtained from Hartree-Fock calculations, whereas the former have been specified semiempirically using a combination of theoretical and experimental information on various finite and infinite systems.

For systems with directional covalent bonds it is important to include a precise description of the electronic orbitals and, accordingly, the embedded-atom method is not applicable here. Instead, we use a parameterized density-functional method [10, 11, 12, 13]. With this method the binding energy is approximated as

$$E_B = \sum_i \epsilon_i - \sum_j\sum_{m_j}\epsilon_{jm_j}^a + \frac{1}{2}\sum_{j\neq k}U_{jk}(R_{jk}). \tag{4}$$

Here, $\epsilon_{jm_j}^a$ is the free-atom single-particle energy of the m_jth orbital of the jth atom, whereas ϵ_i is the single-particle energy of the ith orbital of the system of interest. The latter are obtained from the Kohn-Sham equations

$$\left[-\frac{\hbar^2}{2m_e}\nabla^2 + V_{\rm eff}(\vec{r})\right]\psi_i(\vec{r}) = \epsilon_i\psi_i(\vec{r}). \tag{5}$$

The solutions ψ_i are expanded in a set of atom-centered orbitals

$$\psi_i(\vec{r}) = \sum_p c_{ip}\phi_p(\vec{r}) \tag{6}$$

with p being a compound index that describes the site, the radial dependence, and the angular dependence of the basis function ϕ_p.

The potential $V_{\rm eff}$ of Eq. (5) is approximated through a superposition of free-atom potentials,

$$V_{\rm eff}(\vec{r}) = \sum_j V_j^a(|\vec{r} - \vec{R}_j|), \tag{7}$$

and it is assumed that the matrix elements $\langle\phi_p|V_j^a|\phi_q\rangle$ only then are non-vanishing when at least one of the functions ϕ_p and ϕ_q is centered on $\vec{R}_j$.

With these approximations the Hamilton and overlap matrix elements can be calculated once and for all as a function of interatomic distance through calculations on diatomic molecules once the basis functions have been specified (we use Slater-type orbitals). Finally, the pair potentials U_{jk} of Eq. (4) are obtained by requiring that results of parameter-free density-functional calculations on the diatomics are reproduced accurately.

3. ELEMENTAL METAL CLUSTERS

Metal clusters M_N with M being a simple metal like Na, K, Rb, Cs have attracted considerable attention during the last two decades since the discovery of so-called magic numbers (for reviews, see [14, 15]), i.e., values of N for which the clusters are particularly stable. These experimental findings can be explained by a simple shell-filling argument: Considering a spherical jellium and focusing only on the valence electrons, these will occupy orbitals of s, p, d, $\cdots$ symmetry, and for those values of N where these shells are filled a particularly stable system is obtained. These values match those found in experiment.

However, the jellium model represents a simplification that may not be justified for any other metal clusters than those of the simple metals. In addition, for clusters of transition metals it is not obvious how many electrons per atom should be considered as valence electrons. Instead, the embedded-atom method provides a more accurate description (including that of the nuclear positions, which is lacking within the jellium model) although it can be argued that in particular for $3d$ transition metals the approximations behind this method may be inadequate. Despite these considerations we have chosen to use this method for transition-metal clusters, since its simplification allows for the calculation of the total energy for *very* many structures as will be needed for a largely unbiased systematic study of energetical and structural properties of these clusters.

The identification of the magic numbers for these clusters requires good estimates of the lowest total energy for a given N. Experimental information can not be used in determining relevant structures (for a more detailed discussion, see [16]) and, therefore, we need an approach that gives good estimates of the structures and total energies of the global total-energy minimum. We have used the following strategy that partly has been devised as a simple means of simulating an atom-by-atom growth process.

1. For a given N we consider of the order of 500–1000 random start geometries. Close local-energy minima for these are found using a quasi-Newton approach.

2. The structure of the lowest total energy is disturbed by moving randomly a part of the atoms. This is repeated some 300–500 times and the thereby resulting lowest-total-energy structure is kept.

3. These two steps are repeated for a cluster with $N+M$ atoms, where we have found empirically that $M \simeq 5-10$ is useful.

4. Starting with the structure of N atoms we add one atom randomly to the cluster and the

structure is optimized. This is done in total some 300–500 times and leads to a structure for the cluster with $N + 1$ atoms.

5. Step 4 is repeated until the cluster with $N + M$ atoms is obtained.

6. In parallel to the steps 4 and 5, one atom is removed from the cluster with $N + M$ atoms that was found in step 3 and determine the closest total-energy-minimum structure. This is done for each of the $N + M$ atoms one by one and leads to a structure for the cluster with $N + M - 1$ atoms.

7. Step 6 is repeated until the cluster with N atoms is obtained.

8. In total these calculations lead to two sets of optimized structures with the number of atoms ranging from N to $N + M$. Only if no new structures with lower total energies are generated, it is assumed that the structures of the global-total-energy minima have been identified.

We would like to stress that our '*aufbau/abbau*' approach does not guarantee that the global total-energy minima have been identified. Only a complete information about the total-energy surface in the $(3N - 6)$-dimensional space can guarantee this, but this information is without reach for any but the absolutely smallest values of N.

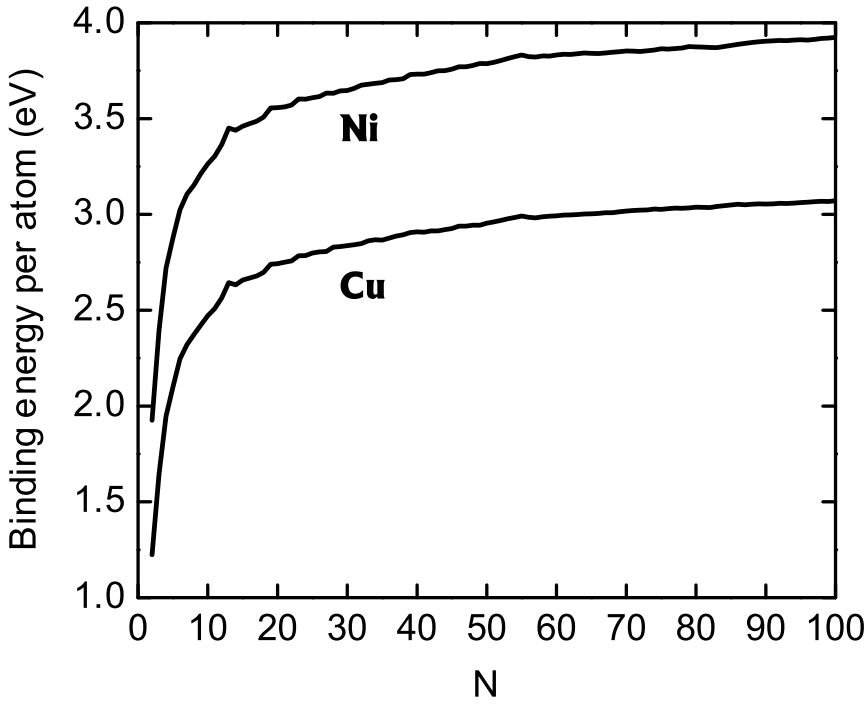

Figure 1: *Optimized binding energy per atom for Ni_N and Cu_N clusters with $2 \leq N \leq 100$.*

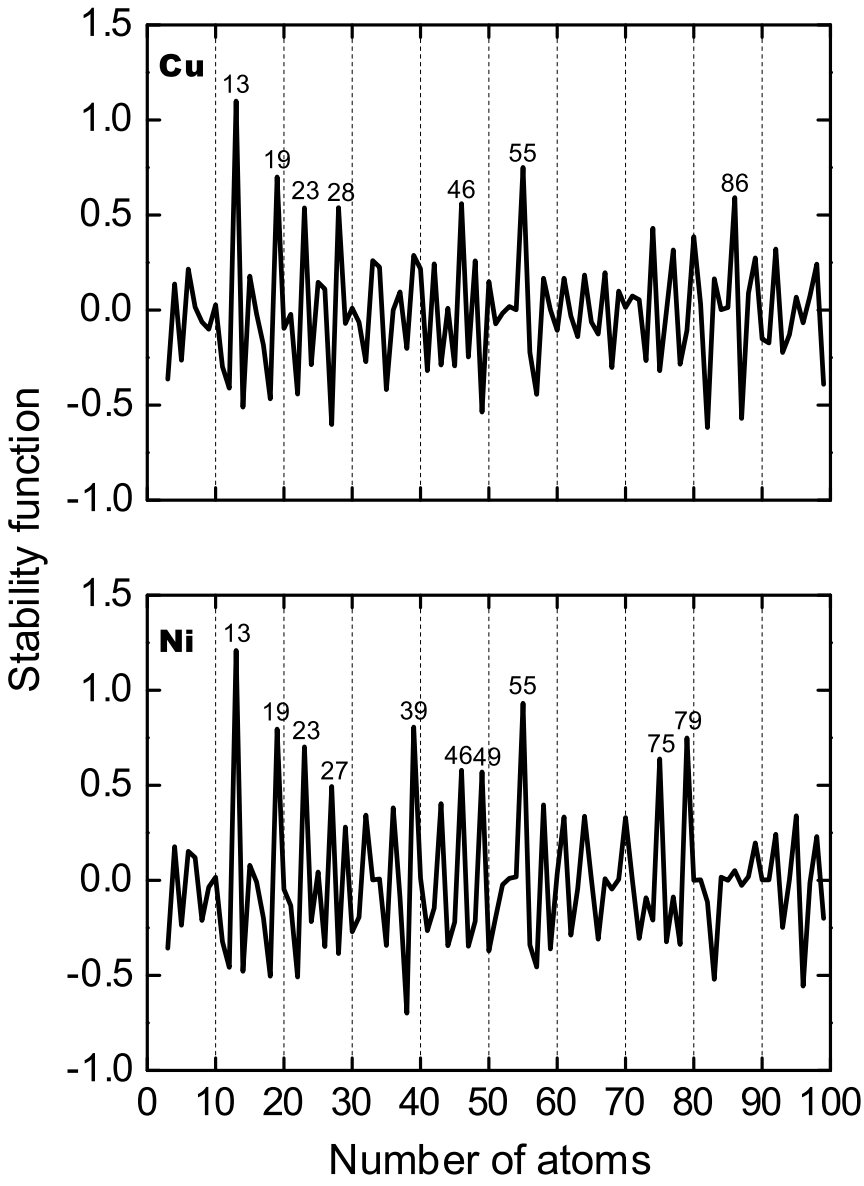

Figure 2: *The stability function for (lower panel) nickel and (upper panel) copper clusters with* $2 \leq N \leq 100$.

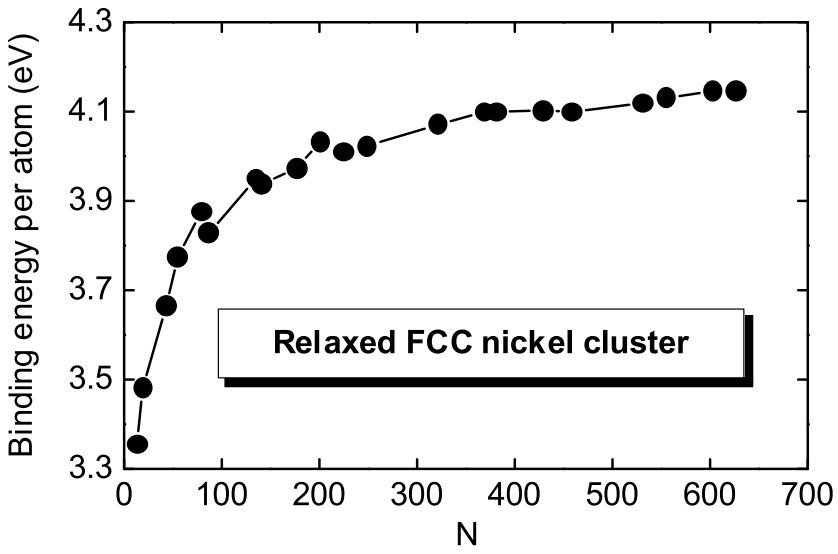

Figure 3: *The binding energy per atom for nickel clusters with* $2 \leq N < 700$. *Compared with Figure 1, here only relaxed finite segments of the FCC crystal structure were considered.*

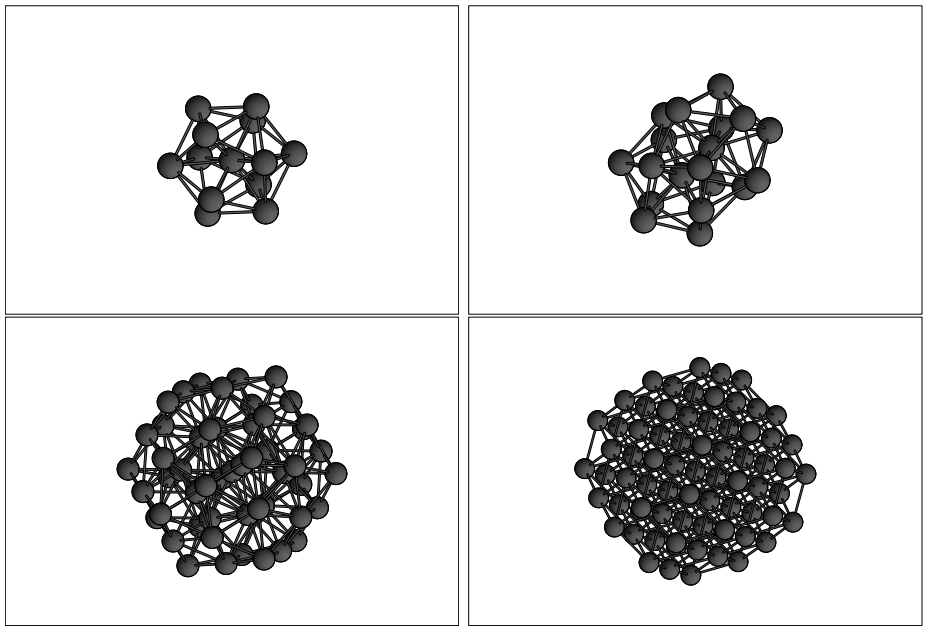

Figure 4: *Optimized structures of* Ni_{13}, Ni_{19}, Ni_{55} *and* Ni_{79}.

As an illustration of the application of our approach we show in Figure 1 the binding energy per atom for clusters of either nickel or copper atoms as a function of N up to $N = 100$. The results show that the binding energy per atoms roughly monotonically approaches the $N \to \infty$ value, although the curves have some structure that suggests the existence of magic numbers. In order to identify these clearly, the stability function

$$S(N) = E_{\rm tot}(N+1) + E_{\rm tot}(N-1) - 2E_{\rm tot}(N) \tag{8}$$

is particularly useful. This has maxima (minima) at particularly stable (unstable) structures and is shown in Figure 2 for the nickel and copper clusters. Comparing the two curves in Figure 2 shows that many magic numbers are similar for the two materials, but also that there are material-specific differences. It should be added at this point, that in [16] we compare our results with the somewhat limited information from more exact studies on smaller systems as well as with other theoretical and experimental information and found a very good agreement.

For $N \to \infty$ one would expect that the Ni clusters have the structure of the FCC crystal structure. We studied also finite segments of the FCC crystal structure obtained by considering spherical parts of the crystal structure with an atom at the center. Thereby, not all values of N can be considered, but, on the other hand, the structure optimization is orders of magnitude simpler thus allowing also systems with larger values of N to be considered. Figure 3 shows the resulting binding energy per atom. It turns out that for $N = 79$ the FCC structure is that of the lowest total energy of Figures 1 and 2. The structure of this system together with those of some smaller clusters are shown in Figure 4.

In contrast to the results obtained by considering only the spherical parts of the crystal structure, those of our '*aufbau/abbau*' approach permits a detailed study of a number of other properties:

1. The radial distribution of the atoms as a function of N. This gives information on whether the clusters grow in a shell-like fashion.

2. Starting with the optimized structures, a harmonic approximation can be used in calculating the vibrational properties.

3. These can in turn be used in calculating specific heat capacities as functions of N and temperature.

4. Through the knowledge of $E_{\rm tot}$ as a function of N for the complete series of N, dissociation channels can be identified.

5. The pair distribution function that is of experimental relevance and that gives information on structural characteristics.

6. The moments of inertia that give information of the overall shape of the clusters.

These studies are currently in progress and their results will be presented later.

4. SEMICONDUCTOR NANOPARTICLES

The existence of directional bonds for typical semiconductors implies that an accurate description of the properties of these materials has to include a treatment of the electronic orbitals. Also when using an efficient parameterized method like the one discussed in Sec. 2, the computational

costs are increased compared with those of the embedded-atom method. Accordingly, it becomes more difficult to carry through detailed structural studies. On the other hand, these directional, often tetragonal, bonds put also certain restrictions on the possible structures.

A further complication is that experimental studies on AB semiconductor nanoparticles often are carried through in some solution and that the nanoparticles often have surfactants that passivate dangling bonds. The fact that the precise size and stoichiometry of those often is not known does not make theoretical studies of their properties easier!

On the other hand, exactly the directional bonds suggest that the structure of the nanoparticles resembles that of the infinite crystal, at least in the inner parts of the nanoparticles. Therefore, as a first approximation one may study finite parts of the crystalline material. This approach is the one we have used in studying more different II-VI and III-V semiconductor nanoparticles and we shall here illustrate the approach by reviewing our results for CdS nanoparticles [17]. We would like to stress that despite these assumptions about the structure, our study represents one of the very few systematic studies of structure-property relations of such materials with more than roughly 50 atoms where structural degrees of freedom have been optimized.

An interesting property of the infinite CdS material is that the wurtzite and zincblende crystal structures are energetically very close [18] which may have interesting consequences for the finite systems. We studied accordingly finite parts of those two crystal structures obtained by considering spheres of different radii with the center at the mid-point of a Cd-S bond. Through this construction only stoichiometric Cd_nS_n nanoparticles are considered.

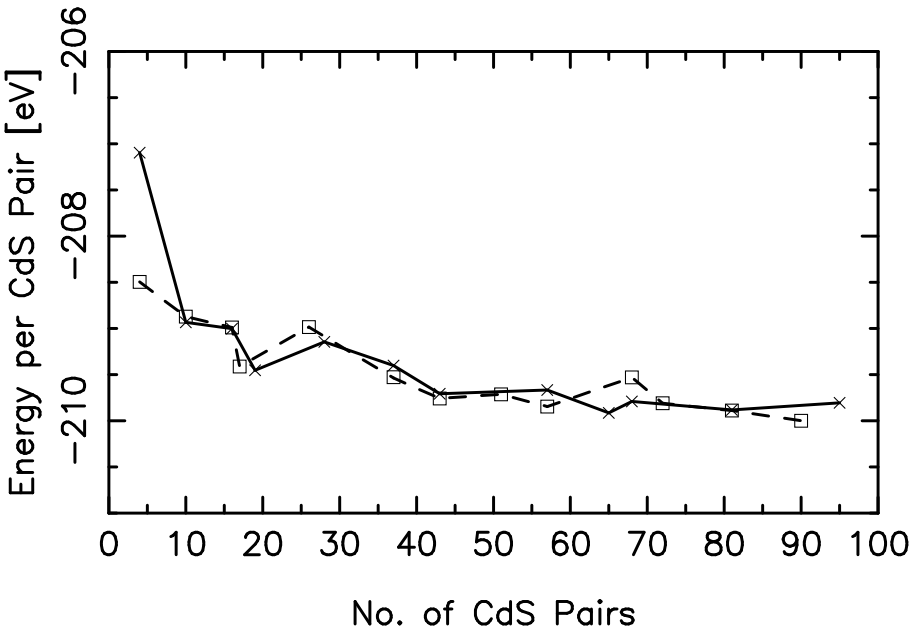

Figure 5: *Variation in the total energy per CdS pair as a function of n for zincblende- (solid curve) and wurtzite-derived Cd_nS_n clusters (dashed curve).*

It turned out (cf. Figure 5) that the relative stability for clusters derived from the two crystal structures in fact was dependent on the size of the system which actually also has been seen in experiment [19]. Further studies on other semiconductor nanoparticles (ZnO, CdSe, InP) have

given similar results.

For each structure the calculation leads to a large amount of information and in order to identify general trends we proceed as follows. First we define the center of the cluster

$$\vec{R}_0 = \frac{1}{N} \sum_{i=1}^{N} \vec{R}_i \tag{9}$$

where the summation runs over the N ($= 2n$ in our case) atoms. Subsequently

$$d_i = |\vec{R}_i - \vec{R}_0| \tag{10}$$

defines the distance of the ith atom to the center. We can then plot various properties as functions of d_i.

As one example, Figure 6 shows the number of atoms as a function of distance to the center both before and after structure relaxation. A Comparison of the two sets of curves for all the different clusters shows that — as expected — structural relaxations are confined to an outer region, whose thickness, moreover, is 2.5–3 Å independent of size and structure of the cluster. Furthermore, it turns out that in this surface region two types of relaxations occur: the metal (Cd) atoms move inward towards the center (the metal atoms seek a high coordination), whereas the sulphur atoms move outward (sulphur atoms are often satisfied with a lower coordination). These differences can not be identified in the curves in Figure 6.

The separation of the system into a bulk and a surface part can also be identified in the electronic properties. E.g., the radial distribution of the Mulliken populations of the valence electrons (cf. Figure 7) shows that in the inner parts these populations deviate only marginally from those of the neutral atoms (i.e., 12 for Cd and 6 for S), but in the surface region the atoms become significantly more ionic.

A further result was that the highest occupied molecular orbital (HOMO) is spread out over the entire cluster independent of n, whereas the lowest unoccupied molecular orbital (LUMO) is confined to the surface region. Therefore, the LUMO is very sensitive to the precise structure of the surface and its energy shows a much more irregular behaviour as a function of n compared to the energy of the HOMO. This also means that surfactants may modify first of all the energy of the LUMO. Excitons play an important role for these nanoparticles, and when assuming that the exciton wavefunction is derived first of all from those of the HOMO and LUMO, our results are in agreement with experimental findings that relaxation processes take place at low-symmetry sites, e.g., at the surface [20].

An interesting observation (Figure 8) is that there is a strong correlation between stability and band gap: large band gap implies larger stability. This can to some extent be considered a generalization of the results discussed above for the clusters of simple metals where the jellium model could be applied.

The overall behaviour of the band gap as well as of the total energy per atom pair is that they are decreasing as a function of nanoparticle size. The decrease of the band gap is observed experimentally: nanoparticles of different sizes have different colours, and the decrease of the total energy is similar to the results for the metal clusters. On the other hand, the fact that the total-energy curve is structured may imply that the size distribution for experimentally produced

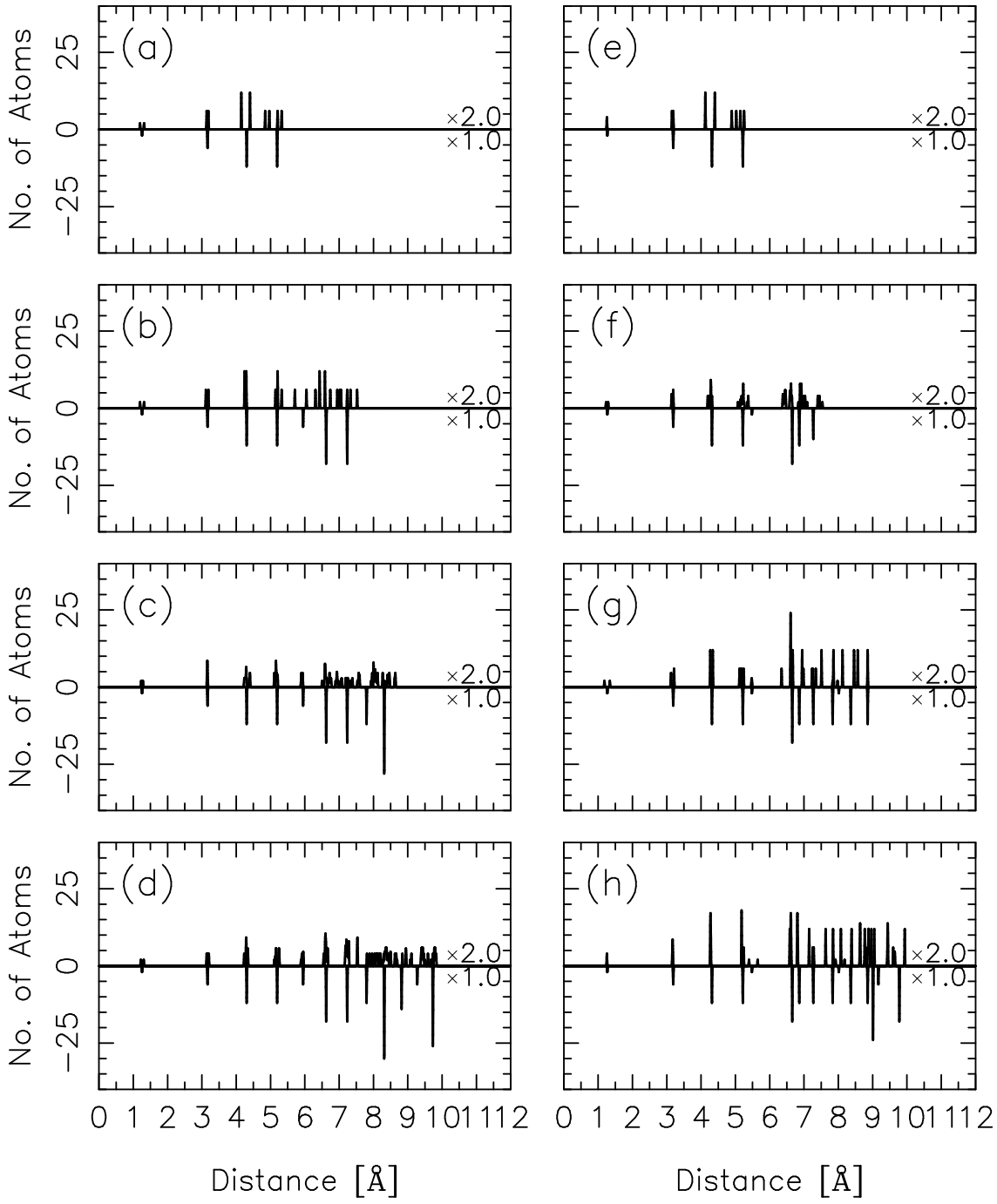

Figure 6: *Radial distribution of the atoms for zincblende- (left column) and wurtzite-derived CdS clusters (right column) with (a),(e) 16, (b),(f) 37, (c),(g) 57, and (d),(h) 81 atom pairs. The curves pointing upwards are for the optimized structures, whereas those pointing downwards are for the unrelaxed structures.*

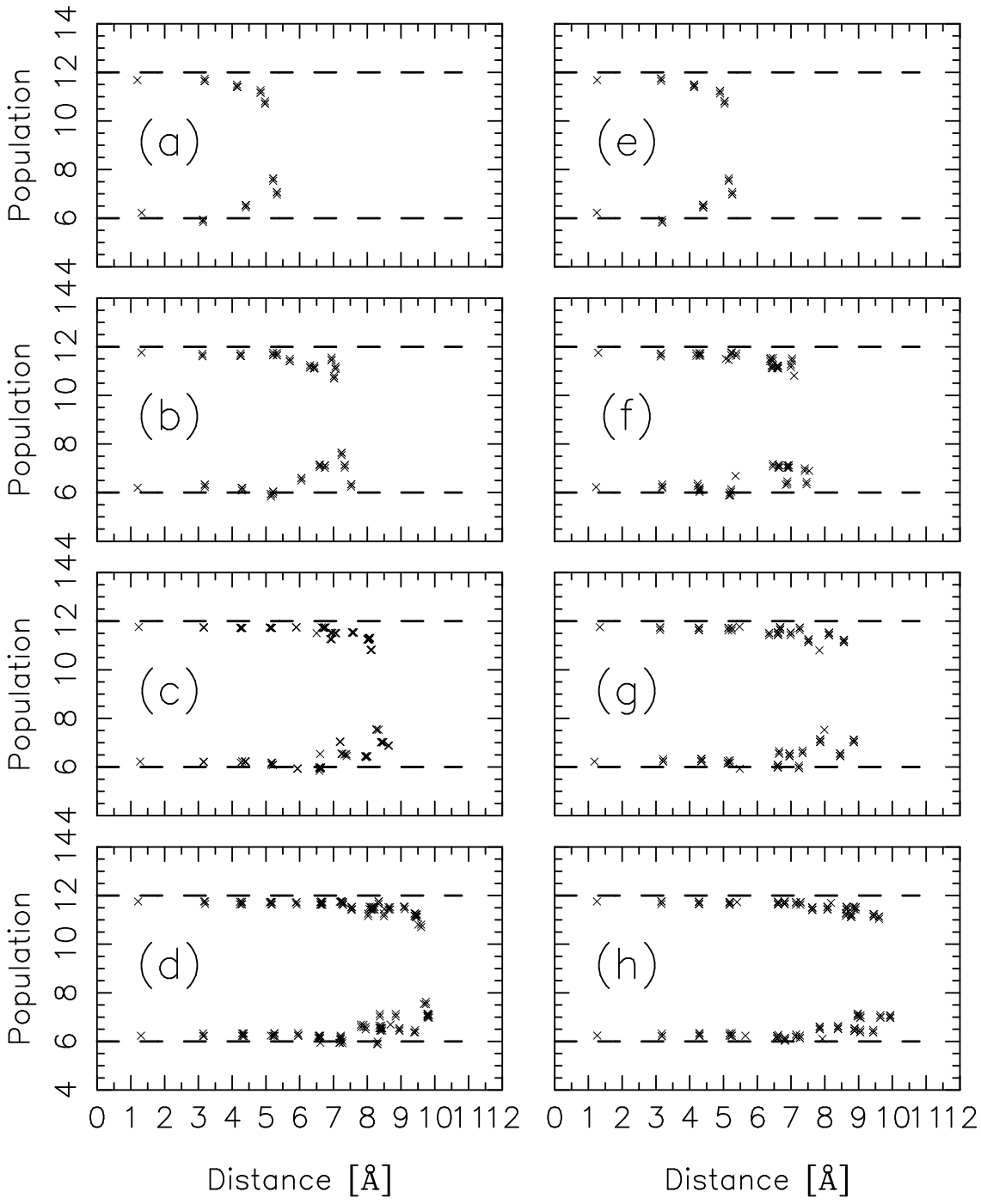

Figure 7: *Radial distribution of the Mulliken populations for zincblende- (left column) and wurtzite-derived CdS clusters (right column) with (a),(e) 16, (b),(f) 37, (c),(g) 57, and (d),(h) 81 atom pairs. The upper parts represent the values for the Cd atoms, and the lower ones those for the S atoms.*

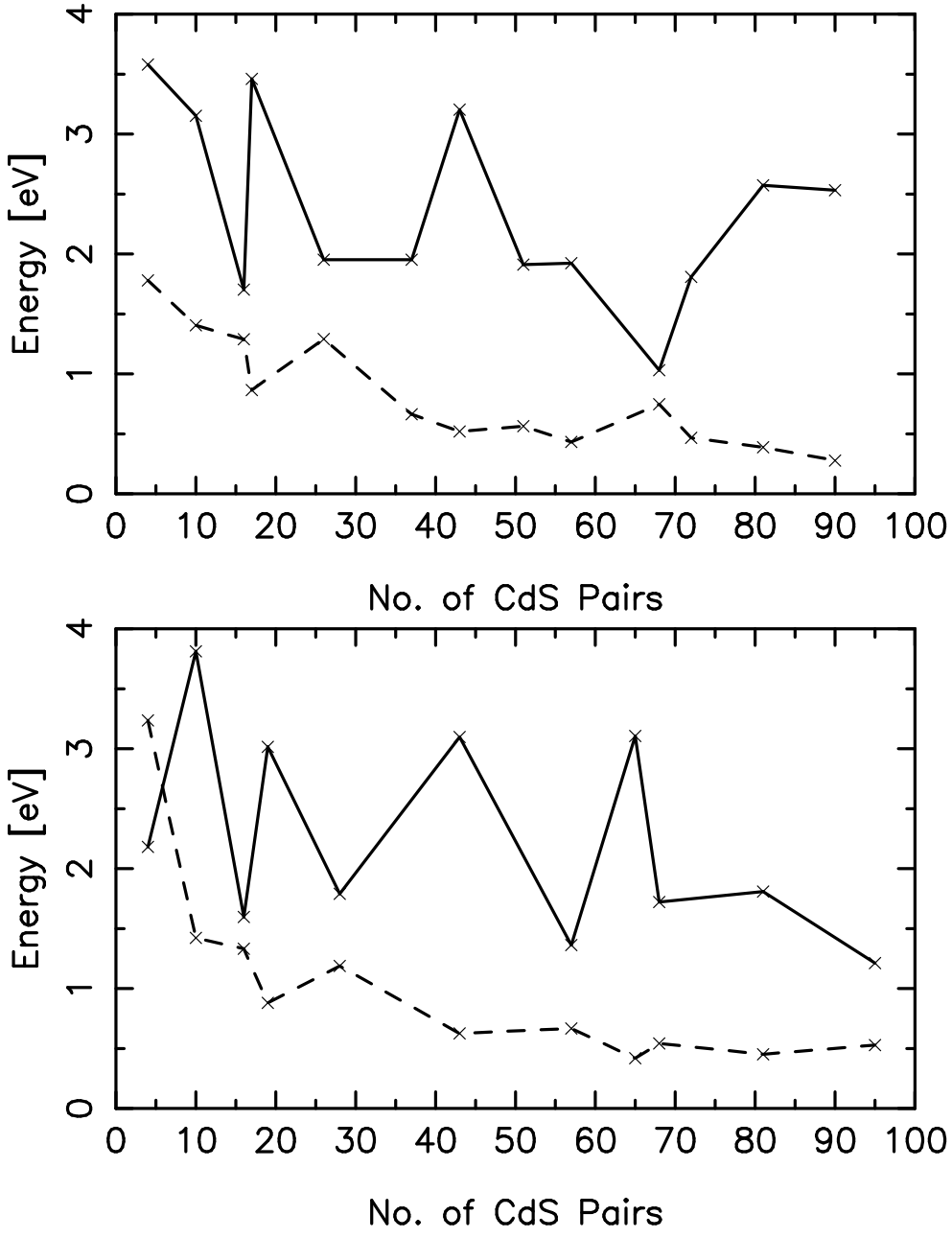

Figure 8: *HOMO-LUMO band gap (solid curve) and relative total energy per atom pair (dashed curve) for (lower part) zincblende- and (upper part) wurtzite-derived CdS clusters.*

samples is less regular than most often is assumed, which in turn could imply that only those clusters for which the stability (and hence band gap) is particularly large are produced. But once again, the presence of surfactants may modify this proposal.

5. METCARS

Let us now return to the materials that were discussed in the Introduction, i.e., the so-called metcars. Since these have directional bonds (for instance between the carbon atoms), the embedded-atom method is inapplicable and we have to use the computationally somewhat more heavy parameterized density-functional method. For a given Ti_mC_n cluster we know essentially nothing about the structure and in order to reduce the search for the global total-energy minimum in the $(3n+3m-6)$-dimensional space we have adapted the methods of genetic algorithms [21, 22]. The general idea behind these methods is that of combining the keeping of 'good building blocks' with randomness. This combination leads to a significant reduction in the number of structures for which the total energy shall be calculated but, nevertheless, we estimate that we in many cases need to consider 1–20 million structures.

There exist different variants of the genetic algorithms but let us describe one of those through a simple example. Let us assume we want to optimize the structure of a cluster of 20 identical atoms. We generate, e.g., 8 different structures at random. For each of those, separately, we find the closest local-total-energy minimum resulting in 8 — most likely different — structures. These 8 structures define the so-called parents. From these 8 we form 4 pairs at random. For any pair we cut each of the two clusters in two halves, whereby the directions of the normals to the cutting planes are generated randomly, and interchange one halfpart from each of the two clusters. Also for these so-called children (of which we have 8 in total) the closest local-total-energy minimum structures are calculated. Thereby we have in total 8 parents and 8 children and out of those 16 optimized structures we choose those 8 with the lowest total energy. These 8 define the parents of the next generation of clusters. This process is continued until the lowest total energy does not change any more as a function of generation number. It should be added that in practice one can never be sure that the last criterion is exactly fulfilled!

There are various ways of modifying this basic principle. E.g., instead of interchanging the halves of two clusters, one may consider only a single cluster for which the two pieces outside a random slice in the middle may be interchanged. Furthermore, so-called mutations may be introduced in which some randomly chosen atom may be moved at random with a certain probability.

We have generalized the method so that we can treat clusters with two types of atoms. Having established that the method worked (by studying Lennard-Jones clusters which are computationally easy to treat) we applied it to the metcars [23] and obtained the following results.

In Figure 9 we show the optimized structure of two of those metcars that turned out to have particularly high symmetry and that were aesthetically particularly appealing, i.e., the $(m,n) = (6,10)$ and $(m,n) = (8,12)$ metcars. Whereas the latter is the one that is well-known from experimental and theoretical studies (and in fact has a T_d symmetry as originally proposed by theory), to our knowledge the former plays essentially no role in experiment.

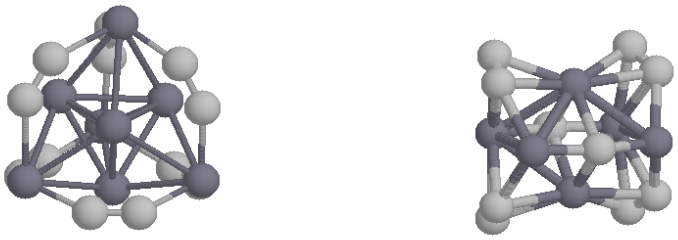

Figure 9: *Optimized structure of (right) Ti_6C_{10} and (left) Ti_8C_{12}. Light (dark) spheres represent C (Ti) atoms.*

The fact that the large abundance of the $(m, n) = (8, 12)$ metcar in experiment is obtained only under certain experimental conditions suggests that not only energetical arguments are required in explaining the special role of the $(m, n) = (8, 12)$ metcar. This is supported by the results presented in Figure 10. Here, we have considered the properties of the whole Ti_7C_n and Ti_8C_n series as functions of n. The energy gain upon addition of a C atom [i.e., $-E_{\rm tot}(\mathrm{Ti}_m\mathrm{C}_n) + E_{\rm tot}(\mathrm{Ti}_m\mathrm{C}_{n-1})$] shows that the $n = 12$ metcar is particularly stable for $m = 7$ but not for $m = 8$. Moreover, the correlation between stability and band gap that we observed for the semiconductor nanoparticles suggests that the $(m, n) = (8, 12)$ metcar is particularly unstable. And, finally, also in the number of nearest-neighbour bonds, the $(m, n) = (8, 12)$ metcar shows no particular properties. Thus, the somewhat disappointing conclusion of our study on the metcars is that total-energy arguments can not explain the experimentally observed large abundance of the $(m, n) = (8, 12)$ metcar but that, most likely, also kinetic effects play a significant role.

6. CONCLUSIONS

In this paper we have discussed the problems related to the determination of the structure of large but finite systems. We emphasized that it is important to identify clearly which properties are of interest in the theoretical studies and, accordingly, whether the structure of a local total-energy minimum, that of the global total-energy minimum, or just some realistic structure is required. Also in the computationally simplest case when 'just some realistic structure' is required, a systematic study of several different systems combined with the size and low symmetry of the individual systems make parameter-free first-principles calculations essentially too involved. Instead of limiting the number of structures and/or systems to very few as well as to impose certain, more or less justified, symmetry constraints we have chosen to use simpler computational methods like the embedded-atom method for metallic systems with delocalized electrons and a semi-empirical tight-binding method for systems with directional chemical bonds and localized electrons.

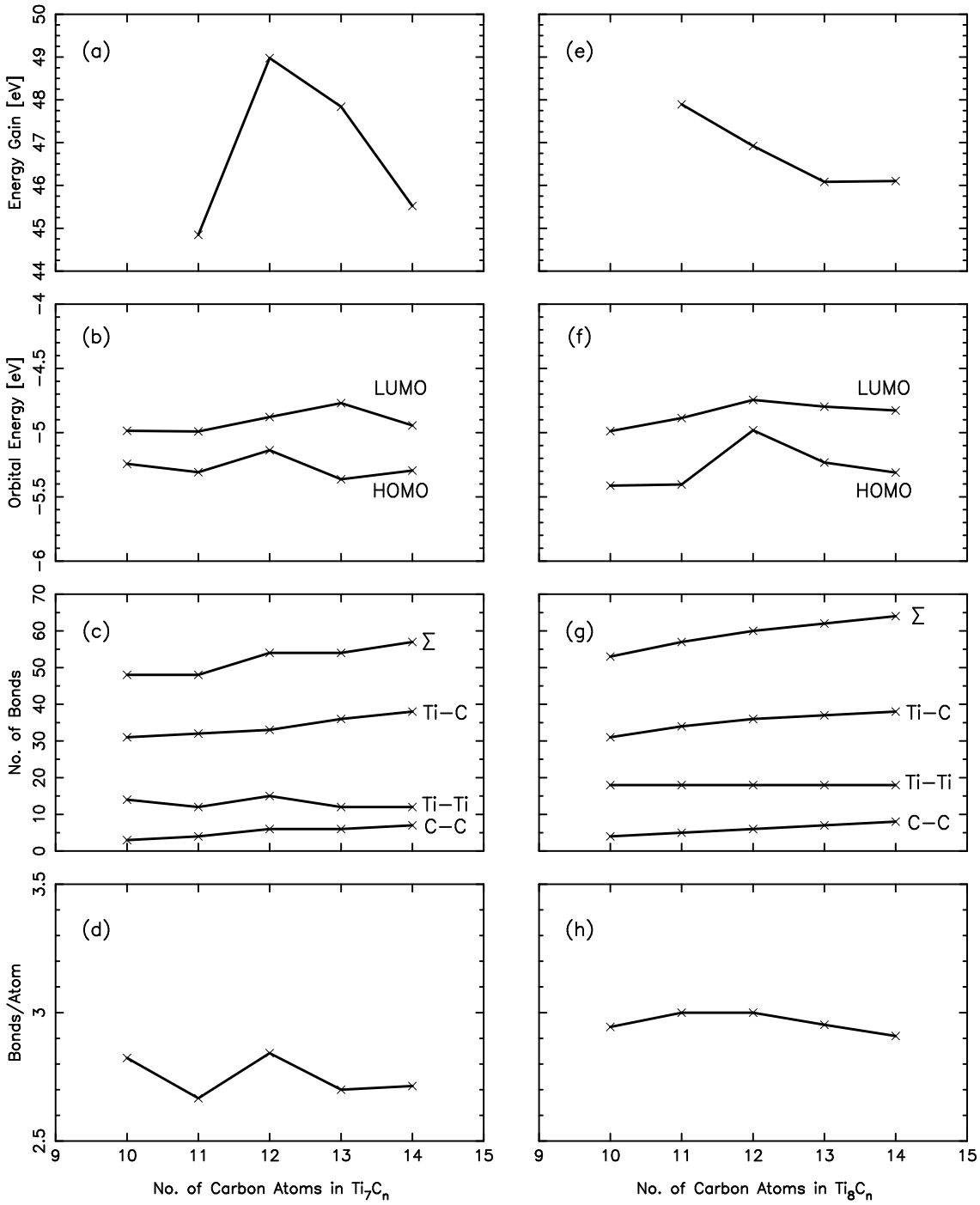

Figure 10: *(a),(e) Energy gain, (b),(f) HOMO and LUMO orbital energies, (c),(g) number of C–C, Ti–Ti, Ti–C bonds and their total number, and (d),(h) total number of bonds divided by total number of atoms for (left) Ti_7C_n and (right) Ti_8C_n as functions of n.*

With these choices we were able to study larger classes of systems systematically. For metallic clusters we presented a largely unbiased '*aufbau/abbau*' method (partly inspired by a simple picture about how clusters are formed in the gas phase) that allowed us to obtain very good candidates for the structures of the global total-energy minima for clusters with up to over 150 atoms. These results, obtained with the embedded-atom method, give immediately information about the so-called magic numbers and are currently been used in obtaining a number of other structural, vibrational, energetical, and thermodynamical properties.

The tight-binding method is computationally somewhat heavier than the embedded-atom method and a systematic study like the one for the metal clusters was only possible if further restrictions were made on the structure. We considered, as one example, stoichiometric CdS nanoparticles derived from either the zincblende or the wurtzite crystal structure. Our results, that we have seen confirmed for other stoichiometric and non-stoichiometric semiconductor nanoparticles, showed a clear size-dependence of the relative stability of the two types of structures. Moreover, we observed a well-defined separation into a bulk and a surface part. Most interesting was a correlation between HOMO/LUMO energy gap and stability as well as the fact that neither of these two quantities was a monotonic function of the size of the system. These results may have important consequences for the size distribution of the experimentally produced nanoparticles.

Finally, the Ti_mC_n metcars represented a class of materials where an essentially unbiased structure optimization was important. To this end we used a variant of the so-called genetic algorithms which was described in some detail. To our surprise the results for the metcars were not able to explain the large abundance of the Ti_8C_{12} metcar that is observed in *some* experiments (depending on the experimental conditions). This we interpret as meaning that this experimental result is determined largely by kinetic effects.

ACKNOWLEDGMENTS

The work behind the present paper was supported by the SFB277 at the University of Saarland and by the DFG through project SP 439/9-1. Moreover, the authors are grateful to Fonds der Chemischen Industrie for very generous support and to Gotthard Seifert, Technical University of Dresden, for numerous useful discussions.

References

[1] B. C. Guo, K. P. Kearns, and A. W. Castleman Jr., Science, **255**, 1411 (1992)

[2] I. G. Dance, J. Chem. Soc., Chem. Commun., **1992**, 1779 (1992)

[3] M. M. Rohmer, M. Bénard, and J. M. Poblet, Chem. Rev., **100**, 495 (2000)

[4] N. Blessing, Diplomarbeit, University of Konstanz, Germany (1998)

[5] C. J. Tsai and K. D. Jordan, J. Phys. Chem., **97**, 11227 (1993)

[6] M. S. Daw and M. I. Baskes, Phys. Rev. Lett., **50**, 1285 (1983)

[7] M. S. Daw and M. I. Baskes, Phys. Rev. B, **29**, 6443 (1984)

[8] S. M. Foiles, M. S. Daw, and M. I. Baskes, Phys. Rev. B, **33**, 7983 (1986)

[9] M. S. Daw, S. M. Foiles, and M. I. Baskes, Mater. Sci. Rep., **9**, 251 (1993)

[10] P. Blaudeck, Th. Frauenheim, D. Porezag, G. Seifert, and E. Fromm, J. Phys. Condens. Matt., **4**, 6389 (1992)

[11] G. Seifert and R. Schmidt, New. J. Chem., **16**, 1145 (1992)

[12] D. Porezag, Th. Frauenheim, Th. Köhler, G. Seifert, and R. Kaschner, Phys. Rev. B, **51**, 12947 (1995)

[13] G. Seifert, D. Porezag, and Th. Frauenheim, Int. J. Quant. Chem., **58**, 185 (1995)

[14] W. A. de Heer, Rev. Mod. Phys., **65**, 611 (1993)

[15] M. Brack, Rev. Mod. Phys., **65**, 677 (1993)

[16] V. G. Grigoryan and M. Springborg, Phys. Chem. Chem. Phys., **3**, 5125 (2001)

[17] J.-O. Joswig, M. Springborg, and G. Seifert, J. Phys. Chem. B, **104**, 2617 (2000)

[18] C. Y. Yeh, Z. W. Lu, S. Froyen, and A. Zunger, Phys. Rev. B, **45**, 12130 (1992)

[19] H. Weller and A. Eychmüller in *Semiconductor Nanoparticles*, edited by P. V. Kamat and D. Meisel, Elsevier Science B.V., Amsterdam (1996)

[20] E. Lifshitz, I. Dag, I Litvin, G. Hodes, S. Gorer, R. Reisfeld, M. Zelner, and H. Minti, Chem. Phys. Lett., **288**, 188 (1998)

[21] J. H. Holland, *Adaption in Natural Algorithms and Artificial Systems*, University of Michigan Press, Ann Arbor (1975)

[22] D. E. Goldberg, *Genetic Algorithms in Search, Optimization and Machine Learning,* Addison-Wesley, Reading, MA (1989)

[23] J.-O. Joswig, M. Springborg, and G. Seifert, Phys. Chem. Chem. Phys., **3**, 5130 (2001)